Journal of Intelligent & Robotic Systems (2018) 92:489–504
https://doi.org/10.1007/s10846-017-0761-9

# An Adaptive Unscented Kalman Filter-based Controller for Simultaneous Obstacle Avoidance and Tracking of Wheeled Mobile Robots with Unknown Slipping Parameters

**Mingyue Cui[1,2] · Hongzhao Liu[1] · Wei Liu[1] · Yi Qin[1]**

Received: 22 November 2016 / Accepted: 5 December 2017 / Published online: 16 December 2017


**Abstract**

A novel unified control approach is proposed to simultaneously solve tracking and obstacle avoidance problems of a wheeled mobile robot (WMR) with unknown wheeled slipping. The longitudinal and lateral slipping are processed as three time-varying parameters and an Adaptive Unscented Kalman Filter (AUKF) is designed to estimate the slipping parameters online More specifically, an adaptive adjustment of the noise covariances in the estimation process is implemented using a technique of covariance matching in the Unscented Kalman Filter (UKF) context. A stable unified controller is applied to simultaneously handle tracking and obstacle avoidance for this WMR system to compensate for the unknown slipping effect. Applying Lyapunov stability theory, it is proved that tracking errors of the closed-loop system are asymptotically convergent regardless of unknown slipping, the tracking errors converge to the zero outside the obstacle detection region and obstacle avoidance is guaranteed inside the obstacle detection region. The effectiveness and robustness of the proposed control method are validated through simulation and experimental results.

**Keywords** Trajectory tracking control · Obstacle avoidance · Slipping parameters estimation · Adaptive unscented Kalman filter · Wheeled mobile robot

## 1 Introduction

All kinds of mobile robots will change our lives in the near future. The relevant environmental information can be obtained by various types of sensors in motion control of a mobile robot [1, 2]. As an important branch of mobile robots, the wheeled mobile robots (WMRs) have better dexterity and larger working space than the traditional industrial robots [3, 4]. Therefore, they are extensively used in complex dynamic environments, such as military scientific and commercial fields and so on [5]. Some control problems on the WMR have been studied by means of neural networks in [6]. Adaptive slipping mode control is usually used to deal with the model uncertainty in the WMR [7]. A radio frequency identification (RFID)-based control method has also been proposed for a mobile robot [8, 9]. Furthermore, the WMR often encounters obstacles when working in complex environment [10]. In this case, some control problems of WMR have been investigated on tracking and obstacle avoidance based on the kinematic model [11–13] We notice that tracking and obstacle avoidance controllers are separately designed in most of the previously existing researches, which easily lead to the low work efficiency and cause high frequency noise [14]. So, it is necessary to design a unified controller to solve simultaneously the two problems–tracking and obstacle avoidance control Furthermore, we notice that these previous works always assume that the mobile robots are subject to a 'pure rolling without slipping', namely they satisfy nonholonomic constraints for controlling mobile robots. However, the slipping effects have a crucial influence on the performance of mobile

✉ Mingyue Cui
cuiminyue@sina.com

[1] College of Mechanical and Electronical Engineering, Nanyang Normal University, Nanyang, Henan 473061, China

[2] Oil equipment intelligent control engineering laboratory of Henan province, Nanyang, Henan 473061, China

robots that cannot be ignored. It means that we should deal with the mobile robot model with slipping induced from perturbed nonholonomic constraints for more practical consideration. From this aspiration, some researchers proposed some approaches for controlling mobile robots considering skidding and slipping [15–19]. Among of them, the lateral slipping effect was only considered in [15, 16]. Wang and Low proposed models of the WMR considering wheel's slipping and analyzed its controllability according to the maneuverability of the WMR in [17] They also designed controllers for path following and tracking of the WMR considering unknown slipping [18, 19]. However, it required that the information of skidding and slipping can be measured by the global positioning system (GPS) and the kinematics was only used for designing the controllers in [9, 18]. What is more, these works [17–19] did not include any ideas for the obstacle avoidance of the WMR with wheels' slipping

For the above reasons, it is very arduous and difficult to handle both the tracking and obstacle avoidance by using one unified controller There are only a few results available on the tracking control problem for the WMR considering obstacle avoidance, even though the problem is practical and important. Recently, some research works have been investigating the problem at the kinematic level [20, 21] and at the dynamic level [22–24]. In [21] that paper considers distributed control of multiple nonholonomic wheeled mobile robots moves along a desired trajectory under the condition that the desired trajectory is available to only a portion of the group of systems. Therefore, the Lyapunov techniques and results from graph theory are applied. Distributed control laws are proposed with the aid of neighbors' information. However, obstacle avoidance and wheels' slipping effects are not considered in the design of the controllers. Some control approaches were reported in that [20, 22] are generally designed for tracking controllers with obstacle avoidance by using position tracking errors without the coordinate transformation. However, some methods were developed without considering skidding and slipping effects [20, 22], and obstacle avoidance is not considered in [23]. In [24], an adaptive controller is designed for trajectory tracking and obstacle avoidance of mobile robots considering unknown slipping at the dynamic level by backstepping technology, but the design process of controller is rather complex and it is very difficult to carry out in practice. These factors above motivate us to further the study on the tracking and obstacle avoidance problems of the WMR in the presence of unknown wheels' slipping

The main contributions of our work are the design of a unified control system for tracking and obstacle avoidance of a class of mobile robots in the presence of unknown slipping at the robot kinematic level Notice that tracking and obstacle avoidance controllers are separately designed in most of the previously existing researches However, an adaptive unscented kalman filter (AUKF) is designed to estimate the slipping parameters in a noisy environment, and provides far greater accuracy than the previous standard unscented Kalman filter(UKF). Different from the extended kalman filter (EKF), the UKF can be applied to approximate the nonlinear process. Therefore, the proposed control strategy is novel in this paper. More specifically, in the theoretical part of this paper, we design a controller that guarantees tracking with bounded error and obstacle collision avoidance for the WMR with unknown wheels' slipping First of all the kinematic model of the WMR considering slipping influence is established, where slipping is modeled as three time-varying parameters. Secondly, the AUKF is applied to estimate online time-varying slipping parameters in a noisy environment. The proposed unified controller is designed by applying the Lyapunov design technique where the angle velocities of the wheels' are considered as the real-time control to deal with the unmatched slipping factor at the robot kinematics level. By using the Lyapunov stability approach with a potential function, we prove that tracking errors of the closed-loop robot system can converge asymptotically, the tracking errors converge to zero outside the obstacle detection region and no collision between the robot and the obstacle is guaranteed inside the obstacle detection region, regardless of unknown slipping. Finally, simulations and experiments are carried out to verify the effectiveness of the proposed control approach.

This paper is organized as follows. In Section 2, we establish the kinematic model of mobile robots considering slipping influence, where slipping is modeled as three time-varying parameters. In Section 3, an AUKF is employed to estimate slipping parameters, which is introduced in details. In Section 4, the control law is designed that guarantees tracking and obstacle avoidance for the mobile robot with slipping, and the stability of the proposed control system is analyzed. Simulation and experimental results are discussed in Section 5. Finally, Section 6 gives some conclusions.

## 2 Kinematic Model of the WMR in the Presence of Slipping

The model of a differentially steered WMR is shown as Fig. 1. It has two driving wheels and two universal wheels where the two driving wheels are powered independently by two direct current motors respectively and have the same wheel radius.

To describe the motion characters of tracked mobile robot simply and rigorously in the general plane motion, a fixed reference coordinate frame $F_1(x_f, y_f)$ and a moving

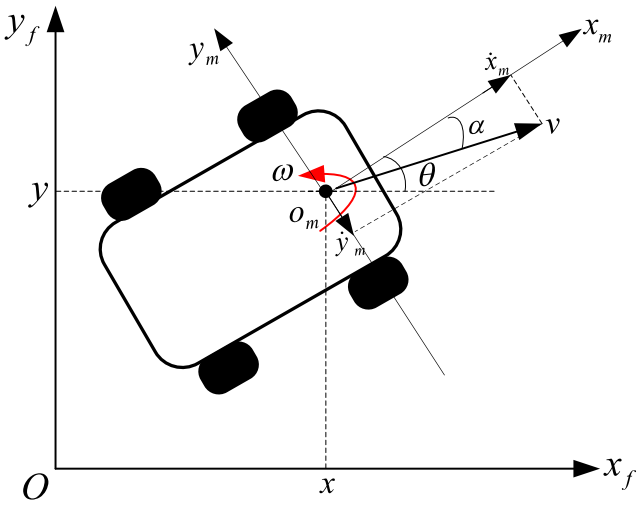


**Fig. 1** Wheeled mobile robot with two independent driving wheels

coordinate frame $F_2(x_m, y_m)$ are defined which attach to the robot body with origin at the geometric center $O_m$

The linear velocities of the left and right driving wheels of the WMR without wheels' slipping are represented as follows

$$v_L = r\omega_L,\ v_R = r\omega_R \tag{1}$$

where $\omega_L$ and $\omega_R$ are the angular velocities of the left and right wheels respectively and $r$ is radius of the wheels. Longitudinal slipping ratio of the left and right wheels of a mobile robot are defined as [25]

$$i_L = \frac{r\omega_L - v_L^s}{r\omega_L},\ i_R = \frac{r\omega_R - v_R^s}{r\omega_R} \tag{2}$$

where $v_L^s$ and $v_R^s$ are the linear velocities of the left and right wheels of the mobile robot with wheels' slipping respectively.

The lateral slipping ratio of a WMR is defined as [25]

$$\delta = \tan\alpha \tag{3}$$

where $\alpha$ is the lateral slipping angle of a mobile robot (see Fig. 1) It is the angle between the velocity of the mobile robot $v$ and the $x$ axis of a local frame attached to the mobile robot

**Assumption 1** The ranges of longitudinal slip ratios $i_L, i_R$ lie in $\{i\,|i \in R, i \neq 1\}$

**Assumption 2** The lateral slipping angle $\alpha$ lies in $\{\alpha\,|\alpha \in R, \alpha \neq \pi/2\}$

**Assumption 3** The reference trajectory is smooth and satisfies the following conditions:

$$|e_3| \neq \frac{\pi}{2}, \alpha - e_3 \neq \frac{\pi}{2} \tag{4}$$

where $e_3 = \theta - \theta_r$ is the orientation error, $\theta$ is orientation angle, $\theta_r$ is reference orientation angle and $\alpha$ is the lateral slipping angle of a mobile robot (See Fig. 1)

*Remark 1* If $i_R = i_L = 1$, from (2), we know that $v_L^s = v_R^s = 0$, which implies a complete slipping, i.e., the wheels of the mobile robot are rotating, while its forward speed is zero, the mobile robot is uncontrollable This case is not considered.

*Remark 2* If $\alpha = \pi/2$, it implies that mobile robot is in a state of complete lateral slipping and the mobile robot is uncontrollable This case is not considered. That is the lateral slipping ratio $\delta$ is bounded.

*Remark 3* Assumption 3 on the reference trajectory implies the following two conditions:

(1) The reference trajectory is such that it does not initiate sharp turns of 90° with respect to the current orientation of the robot.

(2) When Assumption 3 is not satisfied, $\theta_r$ is replaced to solve the singularity problem with the following perturbed version: $\bar{\theta}_r = \theta_r + \bar{\varepsilon}_1$, in which $\bar{\varepsilon}_1 \neq 0$ is some small perturbation value.

*Remark 4* Abrupt changes of the slipping parameter has its obvious physical meaning: the slipping parameter $\delta$ reflects the lateral slipping effect of the WMR, Sudden acceleration of the WMR can directly lead to the sudden changes; Similarly, the slipping parameters $i_R$ and $i_L$ represent the longitudinal slipping of the left and right wheels of robot, slipping parameters $i_R = 0$ or $i_L = 0$ indicates that no slipping occurrence, $i_R > 0$ or $i_L > 0$ indicates accelerated slipping (such as the starting process of robot, or declined ground friction coefficient), and $i_R < 0$ or $i_L < 0$ indicates that decelerated slipping (such as braking process), namely when the robot changes suddenly motion direction and accelerated motion can lead to abrupt changes.

In coordinate frame $F_1(x_f, y_f)$, the kinematic mode of the differential WMR with slipping is described as follows [25]

$$\begin{aligned}\dot{x} &= \frac{r\omega_L(1-i_L)+r\omega_R(1-i_R)}{2}(\cos\theta + \delta\sin\theta)\\ \dot{y} &= \frac{r\omega_L(1-i_L)+r\omega_R(1-i_R)}{2}(\sin\theta - \delta\cos\theta)\\ \dot{\theta} &= \frac{r\omega_R(1-i_R)-r\omega_L(1-i_L)}{b}\end{aligned} \tag{5}$$

where $[x, y, \theta]^{\mathrm{T}}$ is posture vector of the mobile robot, $\theta$ is heading angle of the WMR. We suppose slipping parameters $i_R, i_L$ and $\delta$ are all unknown.

An auxiliary control input is defined as $[v, \omega]^{\mathrm{T}}$, and the relationship between auxiliary control input and real control input $[\omega_L, \omega_R]^{\mathrm{T}}$ is obtained as

$$\begin{bmatrix} v \\ \omega \end{bmatrix} = \begin{bmatrix} \frac{r(1-i_L)\omega_L + r(1-i_R)\omega_R}{2} \\ \frac{-r(1-i_L)\omega_L + r(1-i_R)\omega_R}{b} \end{bmatrix} = T \begin{bmatrix} \omega_L \\ \omega_R \end{bmatrix} \tag{6}$$

where matrix $T$ is a nonsingular matrix, and $T$ is defined as

$$T = r \begin{bmatrix} \frac{1-i_L}{2} & \frac{1-i_R}{2} \\ \frac{-(1-i_L)}{b} & \frac{1-i_R}{b} \end{bmatrix} \tag{7}$$

From (6), we know that the effective control input $[\omega_L, \omega_R]^{\mathrm{T}}$ can be obtained as follows:

$$\begin{bmatrix} \omega_L \\ \omega_R \end{bmatrix} = T^{-1} \begin{bmatrix} v \\ \omega \end{bmatrix} = \frac{1}{r} \begin{bmatrix} \frac{1}{1-i_L} & -\frac{b}{2(1-i_L)} \\ \frac{1}{1-i_R} & \frac{b}{2(1-i_R)} \end{bmatrix} \begin{bmatrix} v \\ \omega \end{bmatrix} \tag{8}$$

Equation (5) can be rewritten as follows:

$$\begin{bmatrix} \dot{x} \\ \dot{y} \\ \dot{\theta} \end{bmatrix} = \begin{bmatrix} \cos\theta + \delta \sin\theta & 0 \\ \sin\theta - \delta \cos\theta & 0 \\ 0 & 1 \end{bmatrix} \begin{bmatrix} v \\ \omega \end{bmatrix} \tag{9}$$

It can be seen from (9) that in order to solve tracking and obstacle avoidance unified control problem of the WMR with unknown slipping parameters, it is the top priority to estimate time-varying slipping parameters online, and then to design unified controller on the basis of estimation results of the slipping parameters.

## 3 A Scheme of the Robotic Slipping Parameter Estimation

Due to the factor that three slipping parameters $i_R, i_L, \delta$ in (5) are not measured directly, it is necessary to estimate slipping parameters in order to design tracking controller. To estimate the states and slipping parameters, joint estimation technique can be used, that is, states and parameters are estimated simultaneously using a same filter [26]. It is often used to solve the state feedback control with uncertain parameters, or the modeling of the parameters with noise and states that can't be measured directly. Because of the incorporation of the states and the parameters, more accurate results may be made using this approach. In the localization of the mobile robot with slipping, the pose and the slipping parameters should be estimated at the same time. A new state vector $\bar{P} = [x, y, \theta, i_R, i_L, \delta]^{\mathrm{T}}$ is defined as a combination of the old states and parametric vector. In this augmented state, the dynamic of the slipping parameters are often unknown. In discrete time domain, it can be rewritten as follows:

$$\bar{P}_{k+1} = \bar{P}_k + w_{\bar{p},k}, k = 0, 1, 2, \cdots \tag{10}$$

where $\bar{P}_k \in R^p$ is the discrete parametric vector; $w_{\bar{p},k} \in R^p$is the additive process noise which drives the model. The UKF is introduced to estimate jointly the state and slipping parameters. Unlike the EKF [27], the UKF is able to approximate the nonlinear process and observation models [28]. Instead, it uses the true nonlinear models and approximates the distribution of the state random variable. The UKF, which does not need to compute the Jacobian, the so-called unscented transform and sigma points are used to propagate all of them through models. We propose an AUKF to estimate slipping parameters of the WMR. More specifically, the values of the process and measurement noise covariances are adaptively adjusted in the estimation process, on the basis of the output pose sequence of the mobile robot model. As a result, the AUKF often leads to more accurate estimations than the standard UKF.

Given the following general nonlinear system

$$\begin{cases} x_{k+1} = f(x_k, u_k) + w_k \\ y_{k+1} = h(x_k) + v_k \end{cases} \tag{11}$$

where $f(x_k, u_k)$ and $h(x_k)$ are the nonlinear process and measurement models of the WMR, respectively. The unmeasurable state vector is represented by $x_k = \begin{bmatrix} x & y & \theta & i_R & i_L & \delta \end{bmatrix}^{\mathrm{T}}$, $u_k$ is known as the control input vector, and $y_k = \begin{bmatrix} \dot{x} & \dot{y} & \dot{\theta} \end{bmatrix}^{\mathrm{T}}$ is the observed output. $w_k$ and $v_k$ are the process and measurement noise, respectively, which are both uncorrelated zero-mean Gaussian white sequences. The initial state vector is defined as $x_0$. The AUKF algorithm is given as follows

**i) Standard UKF**:

(1) Initialization at $k = 0$:

$$\begin{cases} \bar{x}_0 = E[x_0] \\ P_0 = E\left[(x_0 - \bar{x}_0)(x_0 - \bar{x}_0)^{\mathrm{T}}\right] \end{cases} \tag{12}$$

where $\bar{x}_0$ is the expected value of the initial state, $P_0$ is initial covariance.

The augmented state including original states, parameters and process noises are defined as

$$\begin{cases} \hat{x}_0^a = [\, \bar{x}_0^{\mathrm{T}} \;\; 0 \;\; 0 \,]^{\mathrm{T}} \\ P_0^a = diag(P_0, Q_0, R_0) \end{cases} \tag{13}$$

(2) For $k = 1, 2, \cdots, \infty$

(a) Calculate sigma points

$$X_k = \left[\, \hat{x}_k^a, \; \hat{x}_k^a + \gamma\sqrt{P_k^a}, \; \hat{x}_k^a - \gamma\sqrt{P_k^a} \,\right] \tag{14}$$

(b) The prediction step

$$\begin{cases} X^*_{k+1,k} = f(X_k, u_k) \\ \hat{x}^a_{k+1,k} = \sum_{i=0}^{2n} W_i^m X^*_{k+1,k}(i) \\ P^a_{k,k+1} = \sum_{i=0}^{2n} W_i^c \left[X^*_{k+1,k}(i) - \hat{x}^a_{k+1,k}\right]\left[X^*_{k+1,k}(i) - \hat{x}^a_{k+1,k}\right]^{\mathrm{T}} + Q_k \\ X_{k+1,k} = \left[\hat{x}^a_{k+1,k},\ \hat{x}^a_{k+1,k} + \gamma\sqrt{P^a_{k,k+1}},\ \hat{x}^a_{k+1,k} - \gamma\sqrt{P^a_{k,k+1}}\right] \\ Y_{k+1,k} = h(X_{k+1,k}) \\ \hat{y}_{k+1,k} = \sum_{i=0}^{2n} W_i^m Y_{k+1,k}(i) \end{cases} \tag{15}$$

where $Q_k$ is the process noise covariance matrix and the weights $W_i^m$ and $W_i^c$ are defined as follows

$$\begin{cases} W_i^m = \frac{\lambda}{n+\lambda},\ i = 0 \\ W_i^c = \frac{\lambda}{n+\lambda} + (1 - \alpha_F^2 + \beta_F),\ i = 0 \\ W_i^m = W_i^c = \frac{1}{2(n+\lambda)}, i = 1, 2, \cdots, 2n \end{cases} \tag{16}$$

where $n$ is the dimension of the augmented states, $\alpha_F$ controls the size of the sigma point distribution and should be ideally a small number to avoid sampling non-local effects when the nonlinearities are strong and $\beta_F$ is a non-negative weighting term, which can be used to acknowledge the information of the higher order moments of the distribution. For a Gaussian prior the optimal choice is $\beta_F = 2$, and to guarantee positive semi-definiteness of the covariance matrix tuning parameter $\kappa \geq 0$ is chosen. The other parameters are defined as

$$\begin{cases} \lambda = \alpha_F^2(n + \kappa) - n \\ \gamma = \sqrt{n + \lambda} \end{cases} \tag{17}$$

(c) The update step

$$\begin{aligned} P_{yy} &= \sum_{i=0}^{2n} W_i^c \left[Y_{k+1,k}(i) - \hat{y}_{k+1,k}\right]\left[Y_{k+1,k}(i) - \hat{y}_{k+1,k}\right]^{\mathrm{T}} + R_k \\ P_{xy} &= \sum_{i=0}^{2n} W_i^c \left[X_{k+1,k}(i) - \hat{x}^a_{k+1,k}\right]\left[Y_{k+1,k}(i) - \hat{y}_{k+1,k}\right]^{\mathrm{T}} \\ K_k &= P_{xy}P_{yy}^{-1},\ \hat{x}^a_{k+1} = \hat{x}^a_{k+1,k} + K_k(y_{k+1} - \hat{y}_{k+1,k}) \\ P^a_{k+1} &= P^a_{k,k+1} - K_k P_{yy} K_k^{\mathrm{T}} \end{aligned} \tag{18}$$

where $R_k$is the measurement noise covariance matrix.

**ii) Adaptive UKF**

In order to further improve the estimation precision, an adaptive adjustment of the noise covariances in the estimation process is implemented using a technique of covariance matching in the UKF context. More specifically, the adaptive estimation of the process noise covariance $Q$and measurement noise $R$ on the basis of the pose sequence of the mobile robot will be considered. Therefore, $Q$ and $R$ are estimated and updated iteratively from the following [29]:

$$\begin{aligned} Q_k &= K_k C_k (K_k)^{\mathrm{T}} \\ R_k &= C_k + \sum_{i=0}^{2n} W_i^c \left[Y_{k+1,k}(i) - \hat{y}_{k+1,k}\right]\left[Y_{k+1,k}(i) - \hat{y}_{k+1,k}\right]^{\mathrm{T}} \end{aligned} \tag{19}$$

where $\hat{y}_{k+1,k}$ is measured pose of the WMR and $C_k$ is defined as

$$C_k = \sum_{i=k-\bar{L}+1}^{k} E_i (E_i)^{\mathrm{T}} \tag{20}$$

where $E = \left[x - \hat{x}\ \ y - \hat{y}\ \ \theta - \hat{\theta}\right]^{\mathrm{T}}$ are the pose estimation errors of the mobile robot at time step $k$, $C_k$ is an approximation to the covariance of the voltage residual at time step $k$, and $\bar{L}$ is window size for covariance matching. More details can be found in [29, 30].

## 4 Design of the Tracking and Obstacle Avoidance Unified Controller

### 4.1 Potential Function for Obstacle Avoidance

To deal with the obstacle avoidance of the WMR with slipping, we consider the following potential function [31, 32]

$$V_{ob} = \left(\min\left\{0,\ (d_{ro}^2 - L^2)(d_{ro}^2 - l^2)^{-1}\right\}\right)^2 \tag{21}$$

where $l > 0$ and $L > 0$ with $L > l > b > 0$ are radius of the avoidance and detection regions (see Fig. 2), respectively. The parameter $l$ can be chosen by considering the radius of the mobile robot body. The function $d_{ro}$ is

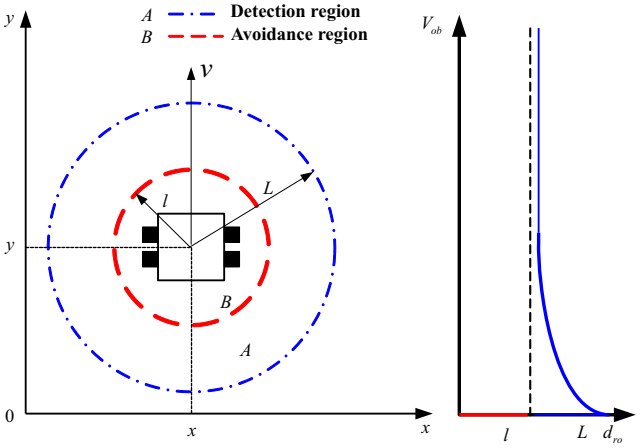


**Fig. 2** Wheeled mobile robot with avoidance and detection region

the distance between the robot and the obstacle, which is defined as

$$d_{ro} = \sqrt{(x - x_o)^2/\alpha_c^2 + (y - y_o)^2/\beta_c^2} \tag{22}$$

where $(x_o, y_o)$ is the position of the obstacle to avoid, $\alpha_c$ and $\beta_c$ are all positive constants. The shapes of the potential function are decided by these two parameters. Therefore, to break the symmetry, different shapes of the potential function for example ellipsoids, can be obtained by choosing different values for the coefficients $\alpha_c$ and $\beta_c$ From (21), we can see the potential function $V_{ob}$ goes to infinity as the boundary of the avoidance region for the mobile robot approaches the obstacle, and is zero outside the detection region.

The first-order partial derivatives of the potential function $V_{ob}$ with respect to the $x$ and $y$ coordinates can be obtained as

$$\frac{\partial V_{ob}}{\partial x} = \begin{cases} \frac{4(L^2-l^2)(d_{ro}^2-L^2)}{\alpha_c^2(d_{ro}^2-l^2)^3}(x - x_o), \text{ if } l < d_{ro} < L \\ 0, \text{otherwise} \end{cases} \tag{23}$$

$$\frac{\partial V_{ob}}{\partial y} = \begin{cases} \frac{4(L^2-l^2)(d_{ro}^2-L^2)}{\beta_c^2(d_{ro}^2-l^2)^3}(y - y_o), \text{ if } l < d_{ro} < L \\ 0, \text{ otherwise} \end{cases} \tag{24}$$

## 4.2 Design of Controller

### 4.2.1 Control objective

Our control objective is to design an adaptive control law for mobile robots with unknown wheels' slipping described by kinematic model (9) so that

1) Outside the detection region ($d_{ro} \geq L$), the mobile robot tracks the reference trajectory generated by the following reference robot:

$$\begin{bmatrix} \dot{x}_r \\ \dot{y}_r \\ \dot{\theta}_r \end{bmatrix} = \begin{bmatrix} \cos\theta_r & 0 \\ \sin\theta_r & 0 \\ 0 & 1 \end{bmatrix} \begin{bmatrix} v_r \\ \omega_r \end{bmatrix} \tag{25}$$

where $x_r y_r$ and $\theta_r$ are the position and orientation of the reference robot, and $v_r$ and $\omega_r$ are the linear and angular velocities of the reference robot, respectively.

2) Inside the detection region ($l < d_{ro} < L$), the mobile robot safely avoids the obstacle under the influence of the reference trajectory $\dot{x}_r = \dot{y}_r = 0$ and $\theta_r = \text{A tan } 2(-E_y, -E_x)$, where $E_x$ and $E_y$ are defined as

$$\begin{cases} E_x = x - x_r + \frac{\partial V_{ob}}{\partial x} \\ E_y = y - y_r + \frac{\partial V_{ob}}{\partial y} \end{cases} \tag{26}$$

This means that as the robot detects an obstacle in its path, it momentarily freezes its reference to the last data received, while trying to resolve the collision. Once it is outside the collision region, it updates the reference to the new values. The reason for this choice is that collision avoidance has a higher priority than tracking, as collision among robots could lead to system damage, which is more critical than temporary degeneration of tracking performance.

**Assumption 4** The reference velocities $v_r$ and $\omega_r$ are bounded, where $v_r > 0$ outside the detection region and $v_r = 0$ inside the detection region.

*Remark 5* Assumption 4 is reasonable because this research focuses on the trajectory tracking problem outside the detection region and to solve the obstacle avoidance problem inside the detection region, respectively.

From $\theta_r = \text{Atan2}(-E_y, -E_x)$, the following can be obtained:

$$\dot{\theta}_r = \frac{E_x \dot{E}_y - \dot{E}_x E_y}{E_x^2 + E_y^2} \tag{27}$$

Accordingly

$$\hat{\dot{\theta}}_r = \frac{E_x \hat{\dot{E}}_y - \hat{\dot{E}}_x E_y}{E_x^2 + E_y^2} \tag{28}$$

where $\hat{\dot{\theta}}_r$ is a smooth estimation of $\dot{\theta}_r$. $\hat{\dot{E}}_x$ and $\hat{\dot{E}}_y$are given as follows [33]

$$\begin{cases} \hat{\dot{E}}_x = \frac{E_x(t+T)-E_x(t)}{T} \\ \hat{\dot{E}}_y = \frac{E_y(t+T)-E_y(t)}{T} \end{cases} \tag{29}$$

where $[t - T, t]$ is a quite short slipping time window. We assume that $\left|\hat{\dot{\theta}}_r - \dot{\theta}_r\right| \leq \varepsilon$ for some small positive $\varepsilon$. Note that most of the variables in $\dot{\theta}_r$ can be measured in fact we have that

$$\left|\hat{\dot{\theta}}_r - \dot{\theta}_r\right| = \frac{E_x(\dot{E}_y - \hat{\dot{E}}_y) - E_y(\dot{E}_x - \hat{\dot{E}}_x)}{E_x^2 + E_y^2} \tag{30}$$

where $E_x$, $E_y$, $\sqrt{E_x^2 + E_y^2}$ can be computed by the state measurements and desired values. So $E_x$, $E_y$ are smooth almost everywhere, we have that $(\dot{E}_x - \hat{\dot{E}}_x) \simeq (\dot{E}_y - \hat{\dot{E}}_y) \simeq o(T)$ and we can choose$\varepsilon \simeq o(T)$ ($o(T)$ denotes higher order infinitesimal of $T$).

### 4.2.2 Design of the unified controller

The tracking errors of mobile robot are defined as $e_1 = x - x_r$, $e_2 = y - y_r$, $e_3 = \theta - \theta_r$. Considering (8) and

the AUKF, the error dynamic equation of the mobile robot is obtained as

$$\begin{bmatrix} \dot{e}_1 \\ \dot{e}_2 \\ \dot{e}_3 \end{bmatrix} = \begin{bmatrix} v[\cos(e_3+\theta_r)+\hat{\delta}\sin(e_3+\theta_r)]-\dot{x}_r \\ v[\sin(e_3+\theta_r)-\hat{\delta}\cos(e_3+\theta_r)]-\dot{y}_r \\ \omega-\dot{\theta}_r \end{bmatrix} \tag{31}$$

In the presence of the slipping, we employ Lyapunov's direct method, and the auxiliary control input is obtained as follows

$$\begin{bmatrix} v \\ \omega \end{bmatrix} = \begin{bmatrix} -k_1\sqrt{E_x^2+E_y^2}(\cos e_3+\delta\sin e_3) \\ -k_2 e_3+\hat{\dot{\theta}}_r \end{bmatrix} \tag{32}$$

where $k_1$ and $k_2$ are positive constants.

However, if the slipping parameters $i_R$, $i_L$ and $\delta$ that appear in (4) are unknown, we cannot choose directly the auxiliary control input as given by (32). Hence, it is necessary to design an AUKF to attain the estimation values of the slipping parameters. If $\hat{i}_L$, $\hat{i}_R$ and $\hat{\delta}$ denote the estimation values of $i_R$, $i_L$ and $\delta$ respectively then from (32), the auxiliary control input can be obtained as follows

$$\begin{bmatrix} v \\ \omega \end{bmatrix} = \begin{bmatrix} -k_1\sqrt{E_x^2+E_y^2}(\cos e_3+\hat{\delta}\sin e_3) \\ -k_2 e_3+\hat{\dot{\theta}}_r \end{bmatrix} \tag{33}$$

where $\hat{\dot{\theta}}_r$ is determined by (28), from (8), actual control input $\omega_L$ and $\omega_R$ can be obtained also by the followings

$$\begin{bmatrix} \omega_L \\ \omega_R \end{bmatrix} = \frac{1}{r}\begin{bmatrix} \frac{1}{1-\hat{i}_L} & -\frac{b}{2(1-\hat{i}_L)} \\ \frac{1}{1-\hat{i}_R} & \frac{b}{2(1-\hat{i}_R)} \end{bmatrix}\begin{bmatrix} v \\ \omega \end{bmatrix} \tag{34}$$

*Remark 6* If $\hat{i}_L = 1$ or $\hat{i}_R = 1$, from (34), we know that actual control input $\omega_L$ or $\omega_R$ will go to infinity. One way to avoid this is by letting $\omega_L$ or $\omega_R$ be replaced by $\omega_{\max}(\omega_{\max}$ of each wheel can achieve a maximum angular velocity).

It can be seen from the above analysis that trajectory tracking and obstacle avoidance yield a unified control principle of the mobile robot with wheels' slipping can be described by the following scheme (See Fig. 3).

#### 4.2.3 Stability analysis of control system

**Lemma 1** *If the real number matrix $A \in R^{n\times n}$ is a positive definite symmetric matrix, then $\forall x \in R^n$ satisfies the following conditions:*

$$\lambda_{\min}(A)\,\|x\|^2 \le x^{\mathrm{T}}Ax \le \lambda_{\max}(A)\,\|x\|^2 \tag{35}$$

*where vector norm $\|x\|$ is defined as $\|x\| = \sqrt{x^{\mathrm{T}}x}$ $\lambda_{\min}(A) > 0$ and $\lambda_{\max}(A) > 0$ denote the minimum eigenvalue and the maximum eigenvalue of the matrix $A$ respectively.*

**Theorem 1** *Consider both system (9) and the reference trajectory described by (25) that satisfies Assumptions 3-4. Also a static obstacle is considered to be avoided that is located at $(x_o, y_o)$. The desired orientation is defined as $\theta_r = \mathrm{A}\tan 2(-E_y, -E_x)$. Then tracking with bounded error outside the detection region, and obstacle avoidance are guaranteed inside the detection region if the control law (33) is applied for all control gains $k_1 > 0$, $k_2 > 0$. Furthermore, the tracking error can be reduced by increasing the value of the control gains.*

*Proof* Consider the error dynamics (31) and control law (33), the closed-loop error dynamics can be obtained as follows

$$\begin{cases} \dot{e}_1 = -k_1\sqrt{E_x^2+E_y^2}(\cos e_3+\hat{\delta}\sin e_3)[\cos(e_3+\theta_r) \\ \qquad +\hat{\delta}\sin(e_3+\theta_r)]-\dot{x}_r \\ \dot{e}_2 = -k_1\sqrt{E_x^2+E_y^2}(\cos e_3+\hat{\delta}\sin e_3)[\sin(e_3+\theta_r) \\ \qquad -\hat{\delta}\cos(e_3+\theta_r)]-\dot{y}_r \\ \dot{e}_3 = -k_2 e_3+\hat{\dot{\theta}}_r-\dot{\theta}_r \end{cases} \tag{36}$$

From the desired orientation angle $\theta_r = \mathrm{A}\tan 2(-E_y, -E_x)$, we have

$$\sin\theta_r = \frac{E_y}{\sqrt{E_x^2+E_y^2}},\quad \cos\theta_r = \frac{E_x}{\sqrt{E_x^2+E_y^2}} \tag{37}$$

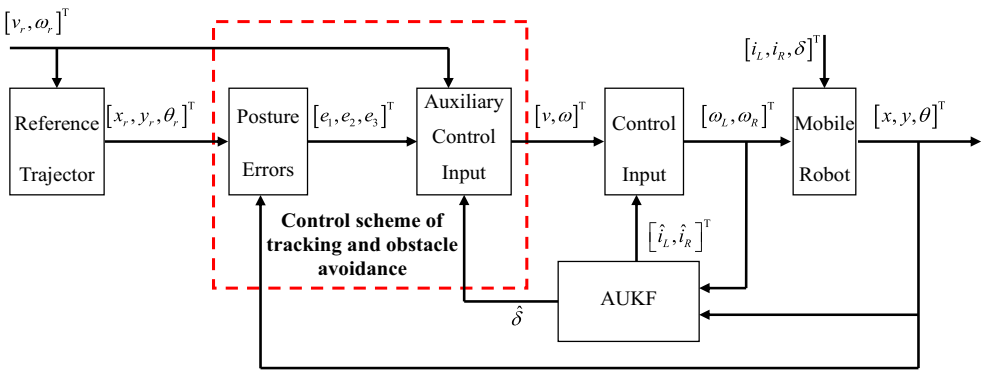


**Fig. 3** Mobile robot trajectory tracking and obstacle avoidance unified control principle scheme

Then, from (36) and (37), (36) can be rewritten as follows

$$\begin{cases} \dot{e}_1 = -k_1(\cos e_3 + \hat{\delta}\sin e_3)[E_x(\cos e_3 + \hat{\delta}\sin e_3) \\ \qquad - E_y(\sin e_3 - \hat{\delta}\cos e_3)] - \dot{x}_r \\ \dot{e}_2 = -k_1(\cos e_3 + \hat{\delta}\sin e_3)[E_x(\sin e_3 - \hat{\delta}\cos e_3) \\ \qquad + E_y(\cos e_3 + \hat{\delta}\sin e_3)] - \dot{y}_r \\ \dot{e}_3 = -k_2 e_3 + \dot{\hat{\theta}}_r - \dot{\theta}_r \end{cases} \tag{38}$$

From (26), we obtain

$$\frac{\partial V_{ob}}{\partial x} = E_x - e_1, \ \frac{\partial V_{ob}}{\partial y} = E_y - e_2 \tag{39}$$

Furthermore, we notice that $\dot{x} = \dot{e}_1 + \dot{x}_r$, $\dot{y} = \dot{e}_2 + \dot{y}_r$

Let us choose Lyapunov-like function candidate as follows

$$V = \frac{1}{2}\left(e_1^2 + e_2^2 + e_3^2\right) + V_{ob} \tag{40}$$

The first-order derivative of the Lyapunov function $V$ is obtained as

$$\dot{V} = e_1\dot{e}_1 + e_2\dot{e}_2 + e_3\dot{e}_3 + \frac{\partial V_{ob}}{\partial x}\dot{x} + \frac{\partial V_{ob}}{\partial y}\dot{y} \tag{41}$$

Substituting (38)-(39) into (41), the following is obtained

$$\begin{aligned} \dot{V} &= e_1\dot{e}_1 + e_2\dot{e}_2 + e_3\dot{e}_3 + (E_x - e_1)(\dot{e}_1 + \dot{x}_r) \\ &+ (E_y - e_2)(\dot{e}_2 + \dot{y}_r) = -k_1(E_x^2 + E_y^2)(\cos e_3 + \hat{\delta}\sin e_3)^2 \\ &- e_1\dot{x}_r - e_2\dot{y}_r + e_3(-k_2 e_3 + \dot{\hat{\theta}}_r - \dot{\theta}_r) \le -k_1(E_x^2 + E_y^2) \\ &(\cos e_3 + \hat{\delta}\sin e_3)^2 - e_1\dot{x}_r - e_2\dot{y}_r - |e_3|\,(k_2\,|e_3| - \varepsilon) \end{aligned} \tag{42}$$

1) When the mobile robot is outside the detection range ($d_{ro} > L$), we have

$$\frac{\partial V_{ob}}{\partial x} = \frac{\partial V_{ob}}{\partial y} = 0 \tag{43}$$

Accordingly, the inequality (42) becomes

$$\begin{aligned} \dot{V} &\le -k_1\left(e_1^2 + e_2^2\right)(\cos e_3 + \hat{\delta}\sin e_3)^2 - e_1\dot{x}_r - e_2\dot{y}_r \\ &\quad - |e_3|\,(k_2\,|e_3| - \varepsilon) \\ &= -\begin{bmatrix} e_1 \\ e_2 \\ e_3 \end{bmatrix}^{\mathrm{T}} A \begin{bmatrix} e_1 \\ e_2 \\ e_3 \end{bmatrix} - \begin{bmatrix} e_1 \\ e_2 \\ |e_3| \end{bmatrix}^{\mathrm{T}} \begin{bmatrix} \dot{x}_r \\ \dot{y}_r \\ -\varepsilon \end{bmatrix} \\ &\le -\begin{bmatrix} e_1 \\ e_2 \\ e_3 \end{bmatrix}^{\mathrm{T}} A \begin{bmatrix} e_1 \\ e_2 \\ e_3 \end{bmatrix} + \left\| \begin{bmatrix} e_1 \\ e_2 \\ e_3 \end{bmatrix} \right\| \left\| \begin{bmatrix} \dot{x}_r \\ \dot{y}_r \\ -\varepsilon \end{bmatrix} \right\| \end{aligned} \tag{44}$$

where $A = \begin{bmatrix} k_1(\cos e_3 + \hat{\delta}\sin e_3)^2 & 0 & 0 \\ 0 & k_1(\cos e_3 + \hat{\delta}\sin e_3)^2 & 0 \\ 0 & 0 & k_2 \end{bmatrix}$,

2-norm $\left\| \begin{bmatrix} e_1 & e_2 & e_3 \end{bmatrix}^{\mathrm{T}} \right\| = \sqrt{e_1^2 + e_2^2 + e_3^2}$

From Assumption 3, we know that $(\cos e_3 + \hat{\delta}\sin e_3)^2 > 0$. Hence, from Lemma 1, we know that $\dot{V} < 0$ for

$$\left\| \begin{bmatrix} e_1 & e_2 & e_3 \end{bmatrix}^{\mathrm{T}} \right\| > \frac{\left\| \begin{bmatrix} \dot{x}_r & \dot{y}_r & \varepsilon \end{bmatrix}^{\mathrm{T}} \right\|}{\lambda_{\min}(A)} \tag{45}$$

where $\lambda_{\min}(A)$ denotes the minimum eigenvalue of matrix $A$. Therefore, the stability of error dynamics, and bounded tracking errors, are guaranteed outside the detection region. Furthermore, the tracking errors can decreased by increasing the control gains $k_1, k_2$

2) When the mobile robot is inside the detection range ($l < d_{ro} < L$), since $\dot{x}_r = \dot{y}_r = 0$, the inequality (42) becomes

$$\begin{aligned} \dot{V} &\le -k_1(\cos e_3 + \hat{\delta}\sin e_3)^2(E_x^2 + E_y^2) - |e_3|\,(k_2\,|e_3| - \varepsilon) \\ &\le -|e_3|\,(k_2\,|e_3| - \varepsilon) \end{aligned} \tag{46}$$

$\dot{V}$ is negative definite, once the following condition is satisfied

$$|e_3| > \frac{\varepsilon}{k_2} \tag{47}$$

Therefore, as shown in reference [20], since $\dot{V}$ is negative definite, $V$ is non-increasing inside the detection region. Since

$$\lim_{\|z - z_o\| \to l^+} V_{ob} = \infty \tag{48}$$

where $z = \begin{bmatrix} x & y \end{bmatrix}^{\mathrm{T}}$, $z_o = \begin{bmatrix} x_o & y_o \end{bmatrix}^{\mathrm{T}}$, then obstacle avoidance is guaranteed. □

*Remark 7* The singularity condition $E_x = E_y = 0$ can occur outside the detection region where

$$\frac{\partial V_{ob}}{\partial x} = \frac{\partial V_{ob}}{\partial y} = 0 \tag{49}$$

which corresponds to $e_1 = e_2 = 0$ and this case can easily be dealt with applying zero controller $v = \omega = 0$

If the singularity condition occurs inside the detection region where the reference direction $\theta_r$ is opposite to the direction vector $\theta$ and they are equal magnitudes, this is a deadlock position. This case can be handled by changing the reference trajectory to drive the robot out of the singularity. We do not investigate this case further in this paper.

## 5 Simulations and Experiments

### 5.1 Simulations

In this section, to validate the effectiveness of the proposed tracking and obstacle avoidance unified control scheme, we perform simulations for trajectory tracking and obstacle avoidance of the WMR in the presence of unknown slipping. We will perform some simulations on the kinematic model of the tracked WMR with slipping using the methods described in previous sections In the simulations, the angular velocities of the two driving wheels are considered as input variables. To observe and compare the simulation

results more easily, we choose two kinds of reference trajectories for the simulations: one is a straight line trajectory, and the other is a circle one. System parameters of the WMR are chosen as follows: In this simulation, we choose the system parameters as $r = 0.125$m, $b$=0.5m. The detection and avoidance radius are $L = 4$m $l = 2$m The filter parameter $\alpha_F$ controls the size of the sigma point distribution and should be ideally a small number to avoid sampling non-local effects when the nonlinearities are strong $\beta_F$ is a non-negative weighting term, which can be used to acknowledge the information of the higher order moments of the distribution, $\gamma$ is a non-negative weighting for $\sqrt{P_k^a}$ in (13), and $\bar{L}$ is window size for covariance matching in (20) The constant filter parameters

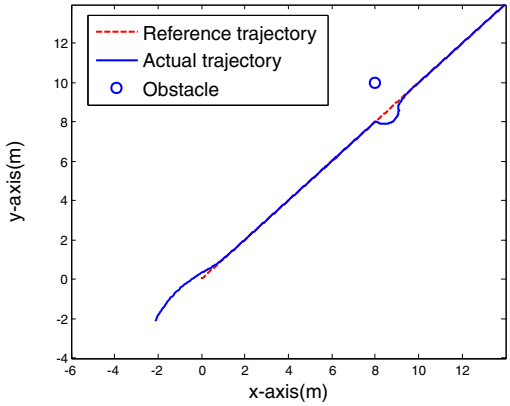


(a) Trajectory tracking and obstacle result

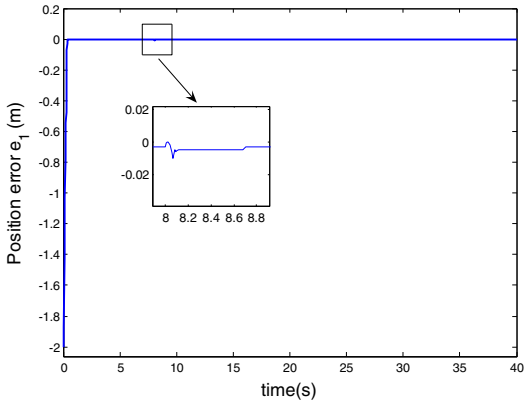


(b) $x$- axis tracking error $e_1$

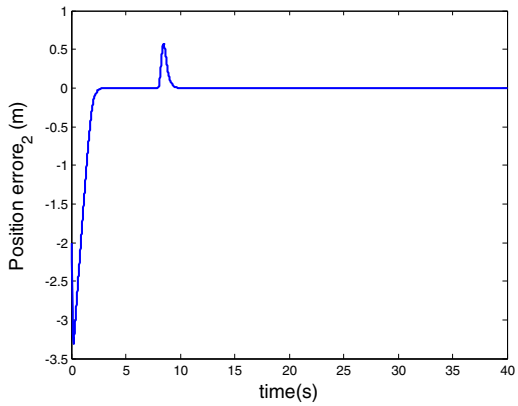


(c) $y$- axis tracking error $e_2$

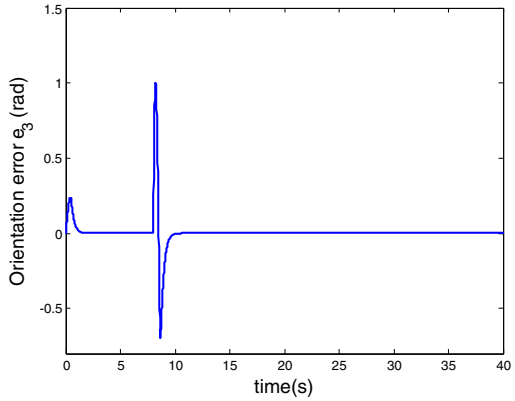


(d) Orientation tracking error $e_3$

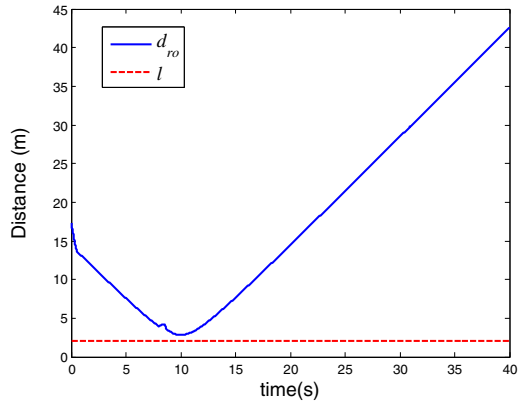


(e) The distance between the robot and the obstacle, and the avoidance region

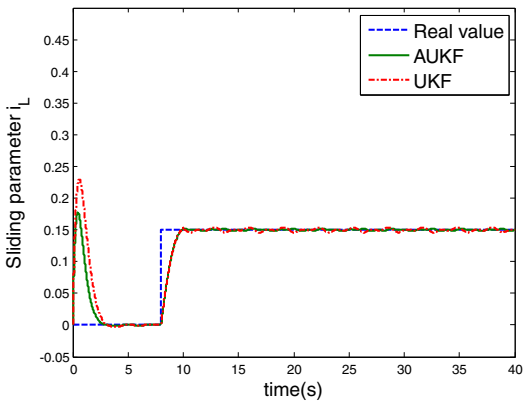


(f) Slipping parameter $i_L$ estimation

**Fig. 4** Simulation results for a straight line reference trajectory in the presence of wheel's slipping

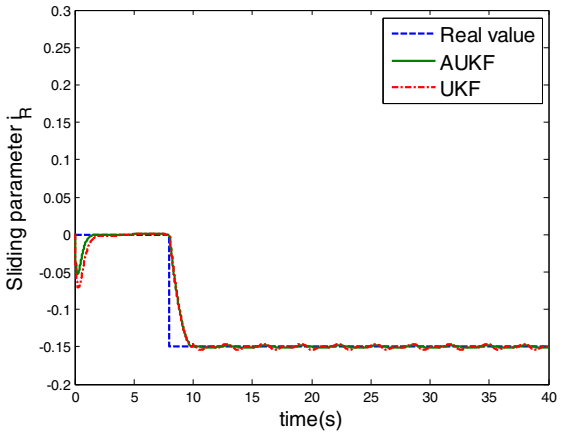


(g) Slipping parameter $i_R$ estimation

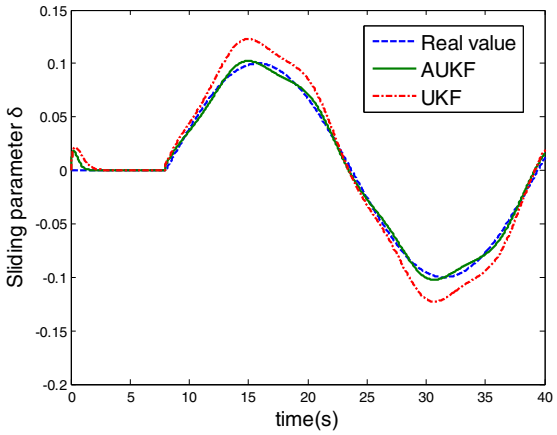


(h) Slipping parameter $\delta$ estimation

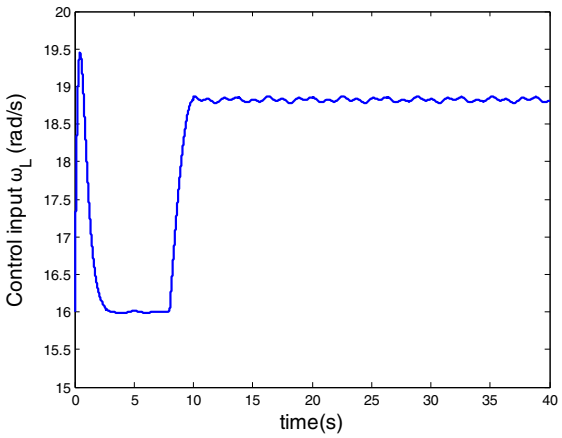


(i) Control input $\omega_L$

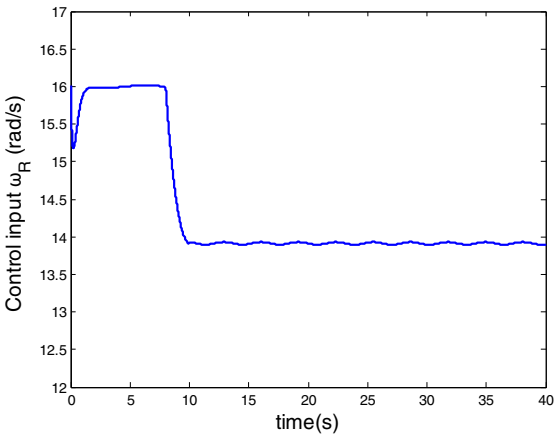


(j) Control input $\omega_R$

**Fig. 4** (continued)

are determined carefully by trialanderror as follows: $\alpha_F = 1$, $\beta_F = 2$, $\gamma = 0$and $\bar{L} = 100$ In (33), the controller gains are chosen through trial-and-error as follows: $k_1 = 50k_2 = 20$.

Note that the kinematic model of the robot is described by the continuous-time (5), (9) and (31). On the other hand, the AUKF is a discrete-time algorithm. Thus, to perform the computer simulation, the continuous-time (5), (9) and (31) are discretized using Euler's forward-difference scheme with a sampling period of $T_s = 0.02s$. Accordingly, the working frequency controller/AUKF is chosen as 50Hz.

**Table 1** Estimation errors of the slipping parameter with UKF and AUKF

| Filters | Slipping Parameters | Maximum | Mean |
|---|---|---|---|
| UKF | $i_L$ | 0.2273 | 0.0032 |
| | $i_R$ | 0.0682 | 0.0033 |
| | $\delta$ | 0.0205 | 0.0042 |
| AUKF | $i_L$ | 0.1774 | 0.0018 |
| | $i_R$ | 0.0465 | 0.0017 |
| | $\delta$ | 0.0052 | 0.0012 |

**Table 2** Estimation errors of the slipping parameter with UKF and AUKF

| Filters | Slipping parameters | Maximum | Mean |
|---|---|---|---|
| UKF | $i_L$ | 0.3997 | 0.0033 |
| | $i_R$ | 0.1398 | 0.0023 |
| | $\delta$ | 0.4897 | 0.0048 |
| AUKF | $i_L$ | 0.3245 | 0.0023 |
| | $i_R$ | 0.1138 | 0.0012 |
| | $\delta$ | 0.2686 | 0.0037 |

**(1) The straight line reference trajectory tracking**

A straight reference trajectory is considered in this example. The initial posture of the reference trajectory is set at

$$\left[\, x_r(0)\ \ y_r(0)\ \ \theta_r(0)\,\right]^{\mathrm{T}} = \left[\, 0\mathrm{m}\ \ 0\mathrm{m}\ \ \tfrac{\pi}{4}\mathrm{rad}\,\right]^{\mathrm{T}}$$

The actual initial posture of the WMR is given as

$$\left[\, x(0)\ \ y(0)\ \ \theta(0)\,\right]^{\mathrm{T}} = \left[\, -2\mathrm{m}\ \ -2\mathrm{m}\ \ \tfrac{\pi}{4}\mathrm{rad}\,\right]^{\mathrm{T}}$$

The reference velocity $v_r = 2\mathrm{m/s}$ and $\omega_r = 0\mathrm{rad/s}$, the reference orientation angle $\theta_r = \pi\,\mathrm{rad}/4$. The obstacle is located at $(x_o, y_o) = (8\mathrm{m}, 10\mathrm{m})$. In order to demonstrate the tracking performance, abrupt changes are simulated to occur in the three slipping parameters at time $t = 8\mathrm{s}$ Three slipping parameters and their initial estimation values are as follows:

$$\left[\, i_L\ \ i_R\ \ \delta\,\right] = \left[\, 0.15\ \ -0.15\ \ 0.1\sin(0.2t)\,\right]$$

$$\left[\, \hat{i}_L(0)\ \ \hat{i}_R(0)\ \ \hat{\delta}(0)\,\right] = \left[\, 0\ \ 0\ \ 0\,\right]$$

The slipping parameters of the mobile robot contain Gaussian white noise, their amplitudes lie within in $[-0.1, 0.1]$.

The straight line trajectory tracking and obstacle avoidance results of the proposed control strategy are presented in Fig. 4. From Fig. 4a we know that the proposed control method can conquer the effect of slipping while the obstacle avoidance is guaranteed. Tracking errors of the controlled robot system are shown in Fig. 4b-d Observe that the tracking errors converge asymptotically to zeroes except in the range that the mobile robot detects the obstacle and when the wheels' slipping occurs In addition, the distance between the robot and obstacle is shown in Fig. 4e From this figure, notice that this distance is always larger than the avoidance radius $l = 2\mathrm{m}$, that is to say there is no collision between the robot and the obstacle. Meanwhile, the obtained result for slipping parameters estimation with AUKF is shown in Fig. 4f-h The result is also compared with the standard UKF, which is shown in Fig. 4f-h and Table 1 The estimation errors are shown in Table 1. It is

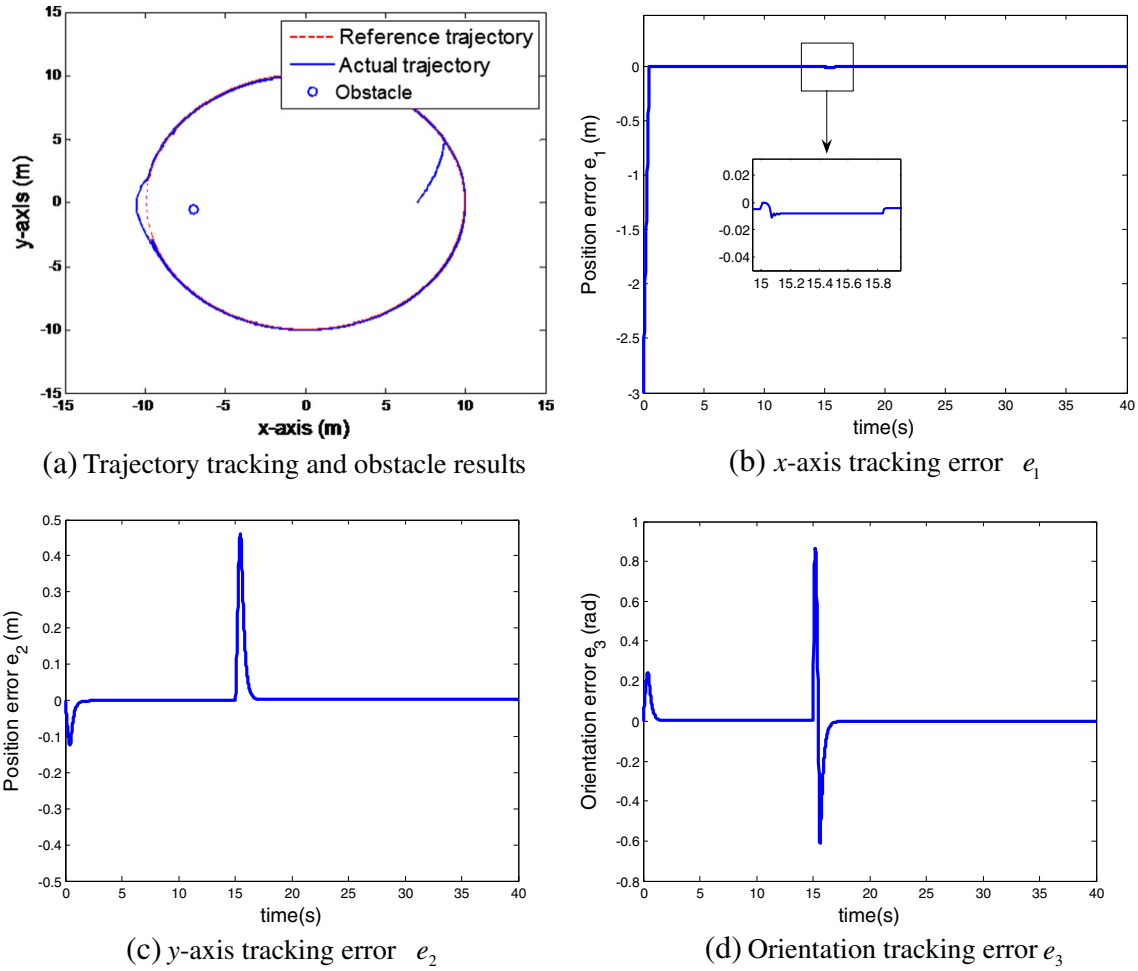


(a) Trajectory tracking and obstacle results

(b) $x$-axis tracking error $e_1$

(c) $y$-axis tracking error $e_2$

(d) Orientation tracking error $e_3$

**Fig. 5** Simulation results for a curved line reference trajectory in the presence of wheels' slipping

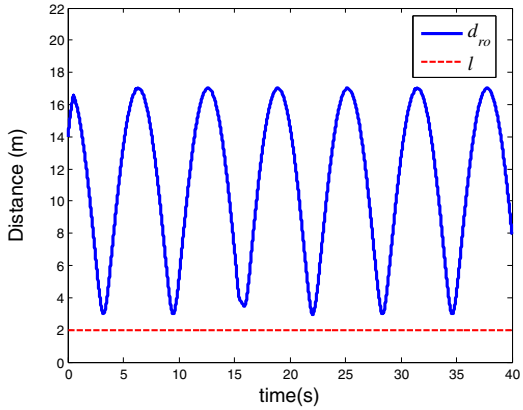


(e) The distance between the robot and the obstacle, and the avoidance region

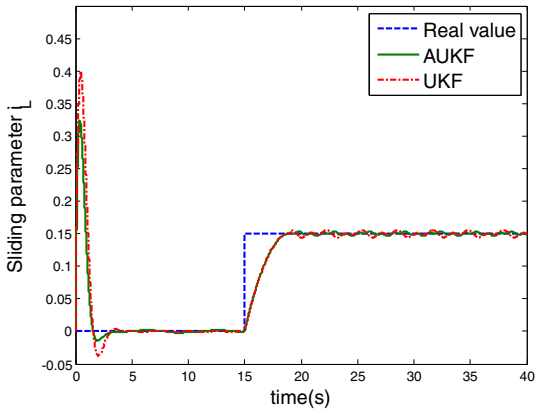


(f) Slipping parameter $i_L$ estimation

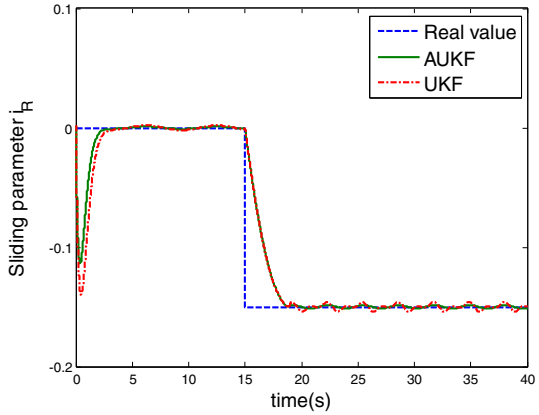


(g) Slipping parameter $i_R$ estimation

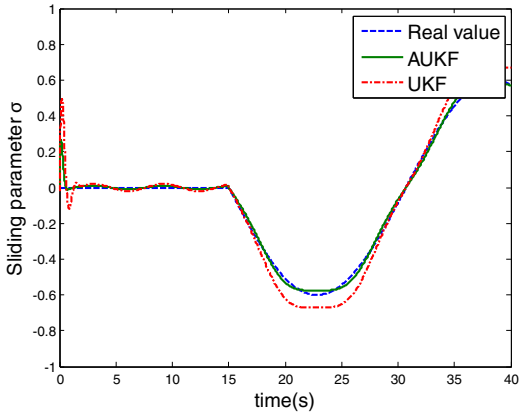


(h) Slipping parameter $\delta$ estimation

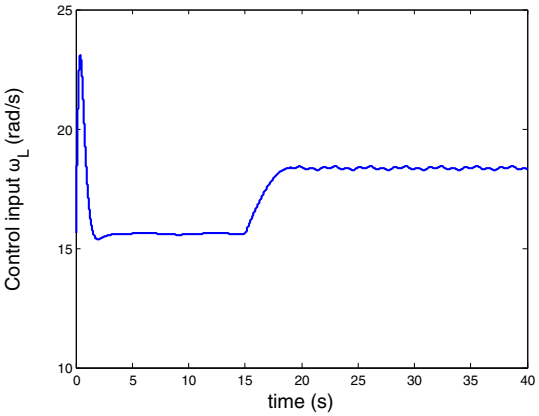


(i) Control input $\omega_L$

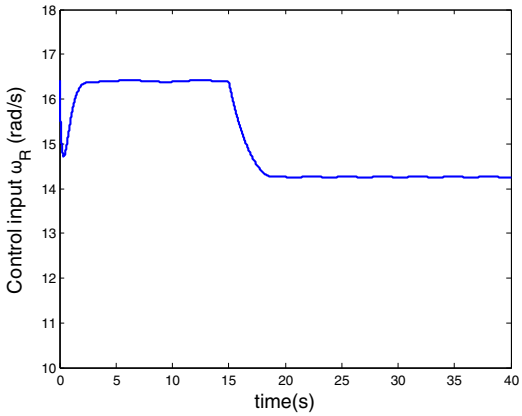


(j) Control input $\omega_R$

**Fig. 5** (continued)

clear that the AUKF-based algorithm can estimate three slipping parameters as well as the pose of the robot more accurately, compared with the standard UKF. Additionally, Table 1 shows that the maximum absolute error of the AUKF algorithm and the absolute mean error are all much smaller than the UKF algorithm. In the presence of robot wheel's slipping, the control input $\omega_L$ and $\omega_R$ are shown in Fig. 4i-j

**(2) The curved line reference trajectory tracking**

In this case, we consider a curved line reference trajectory generated by reference velocities $v_r = 2$m/s and

$\omega_r = 0.2$rad/s for $0 \leq t \leq 40$. The equation of the straight line reference trajectory is given as

$$\begin{cases} x_r = 2\cos t \\ y_r = 2\sin t \end{cases}$$

In addition, it is assumed that the obstacle is located at $(x_o, y_o) = (-7, -0.5)$. The initial postures of the reference trajectory and the actual mobile robot are chosen as

$$\left[\, x_r(0) \;\; y_r(0) \;\; \theta_r(0) \,\right]^{\mathrm{T}} = \left[\, 10\mathrm{m} \;\; 0\mathrm{m} \;\; \tfrac{\pi}{4}\mathrm{rad} \,\right]^{\mathrm{T}}$$

The actual initial posture of the WMR is

$$\left[\, x(0) \;\; y(0) \;\; \theta(0) \,\right]^{\mathrm{T}} = \left[\, 7\mathrm{m} \;\; 0\mathrm{m} \;\; \pi\mathrm{rad}/4 \,\right]^{\mathrm{T}}$$

The wheel's slipping is described as

$$\left[\, i_L \;\; i_R \;\; \delta \,\right] = \left[\, 0.15 \;\; -0.15 \;\; 0.6\cos(0.2t) \,\right]$$

which influences the mobile robot after $t = 15$s.

In order to facilitate comparison of the simulation results, the control system parameters, control parameters and the parameters of the AUKF are all the same as in the previous simulations in the case of straight line reference path tracking

In the case of tracking a circle reference trajectory the simulation results are shown in Fig. 5 where the proposed control strategy can compensate the slipping effects and has good performance of obstacle avoidance (see Fig. 5a-d). Additionally, Fig. 5e reveals that there is no collision between the robot and obstacle Fig. 5f-h and Table 2 show that the three slipping parameters can be estimated more accurately in real time by the AUKF compared with the standard UKF In the presence of robot wheel's slipping, the control input $\omega_L$ and $\omega_R$ are shown in Fig. 5i-j

Furthermore, from Figs. 4 and 5, we can further find that the proposed control method can avoid static obstacles and effectively conquer the wheels' slipping effect for the given trajectory tracking of the mobile robot This is mainly because the designed tracking controller has adaptive ability, whose slipping parameters are estimated in real time. Moreover, even if the wheels' slipping parameters change suddenly, the AUKF can still exactly estimate slipping parameters in real time to satisfy the demands of the robot in the actual working environment. Consequently, the unified control algorithm for tracking and obstacle avoidance has good robustness and adaptive ability to cope with slipping parameter perturbations of the mobile robot.

## 5.2 Experimental Results

In order to demonstrate the effectiveness and applicability of the proposed method, a real-time control system is implemented for the mobile robot. In the experiment, a mobile robot with one vision navigation system fixed on the top moves along the marking line. Figure 6 shows the

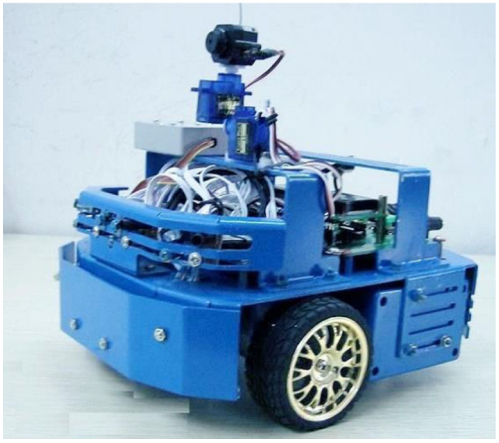

**Fig. 6** Mobile robot in real experiment

picture of the robot which is used in the experiment. It has the same structure as Fig. 7, with two driving wheels and two passive wheels. The diameter of the robot is 50cm and the radius of driving wheel is 12.5cm. The driving wheels are driven by motors with the maximum permissible speed of 3900n/min. The motor and the driving wheel are connected by a reduction gears box. For convenience of comparison the parameters of the control law and AUKF are all the same as the simulations.

The control board of the mobile robot consists of the main controller and motor controller. The main controller of the robot is dsPIC30F6014, which is running at 32MHz. It is used to communicate with host computer and motor controller. It receives the voltage instruction from the host computer and calculates the voltage distribution on the right and left motors, respectively, and then sends the data through SPI communication to the auxiliary motor controller, dsPIC4012. The motor controller generates a PWM signal with different duty cycles according to the voltage instruction.

In the real experiment, the obstacles are detected by ultrasonic sensors. On one hand, the actual position (include the orientation angle $\theta$) measure of the mobile robot are

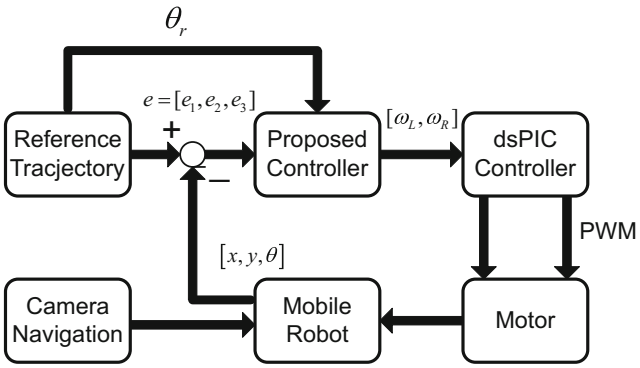


**Fig. 7** Schematic diagram of the experiment control System

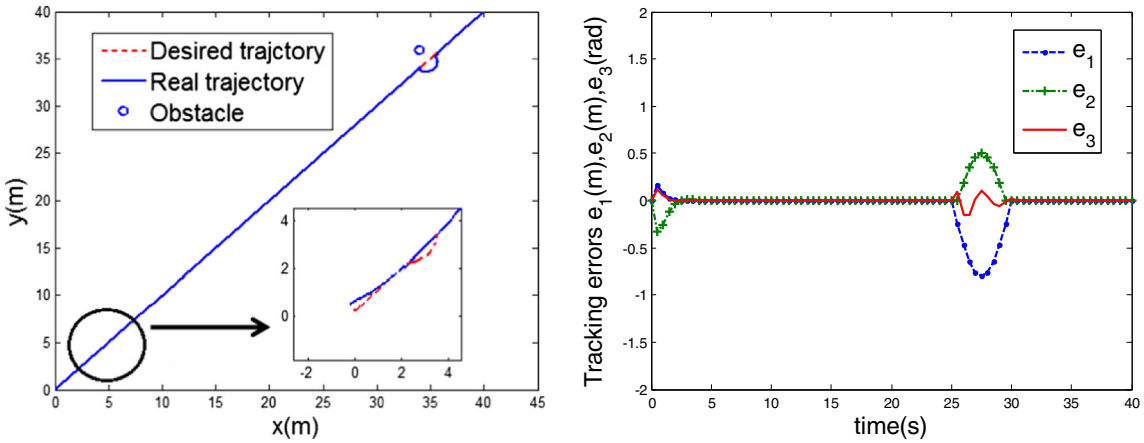


(a) Trajectory tracking and obstacle results (b) Tracking errors

**Fig. 8** Experimental results for the straight-line tracking errors with initial error (0m, 0m, rad)

reconstructed by using the photoelectric encoders, which samples the left and right wheel velocities to calculate the current robot configuration. On the other hand, the position measure would be not accurate due to the slipping between the robot and the ground. So the orientation angle is necessary to be obtained by the camera navigation system to amend the orientation angle $\theta$ measured by the photoelectric encoders.

Figure 7 shows the whole schematic diagram of the trajectory tracking system for the mobile robot. Because of the complexity of the calculation process, the proposed adaptive tracking controller based on AUKF is carried out in the main computer running at the frequency of 1.86MHz. The software for implementing the algorithm is developed in Visual C++2015. After the reference trajectory has been set up, the proposed adaptive tracking controller generates the real voltage instruction. The dsPIC controller can generate the PWM signal to control the velocity of the mobile robot so that the mobile robot moves according to the instruction. The vision navigation system evaluates the posture of the robot and feedback the information to the host computer until the posture error is minimized.

In order to validate the applicability of the proposed control scheme, the mobile robot was required to track reference trajectories of a straight line in an obstacle environment. The real position of the mobile robot is fed back to the mobile robot every 0.05 second by a camera navigation system. In the straight-line tracking the reference velocities are given as $v_r = 2$m/s $\omega_r = 0$rad/s The robot started tracking with initial errors $e_1$=0m, $e_2$=0m and $e_3$=0° At $t = 2$s, the arbitrary external wheels' slipping disturbance is fed into the robotic system by laying sand on the ground and the sand on the ground is located at (2.5m, 2.5m). The actual initial posture of the WMR is located

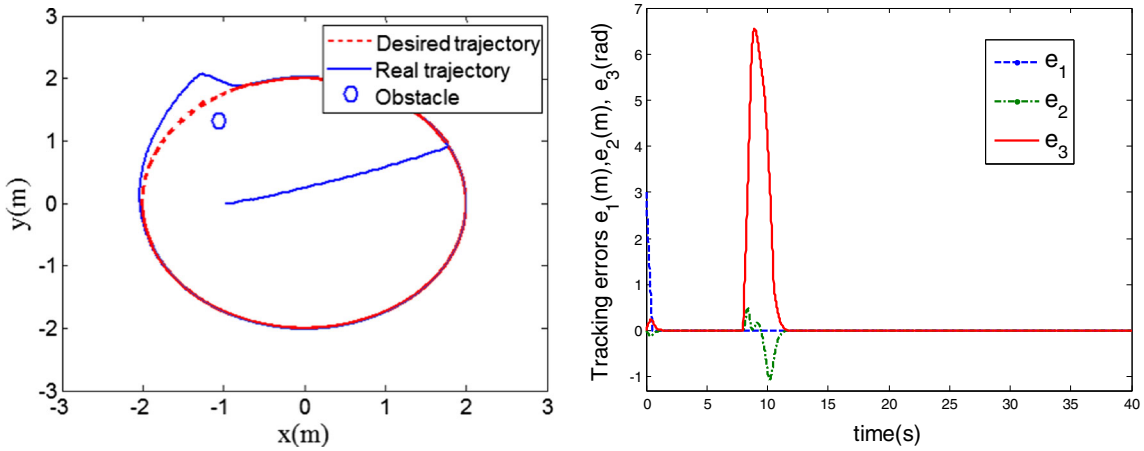


(a) Trajectory tracking and obstacle results (b) Tracking errors

**Fig. 9** Experimental results for the circular trajectory tracking errors with initial error (-3m, 0m, rad)

at $[x(0), y(0), \theta(0)] = [0\text{m}, 0\text{m}, 45°]$ and the obstacle is located at $(x_o, y_o) = (34\text{m}, 37\text{m})$. The detection radius is $L = 4\text{m}$, and the avoidance radius is $l = 1.5\text{m}$ In the circular trajectory tracking the reference velocities are given as $v_r = 2\text{m/s}$ $\omega_r = 0.20\text{rad/s}$. The robot started tracking with initial errors $e_1 = -3.0\text{m}$, $e_2$=0m and $e_3$=0°. The arbitrary external wheels' slipping disturbance is fed into the robotic system by laying sand on the ground, and the sand on the ground is located at (-1.0m, 1.0m). The actual initial posture of the WMR is located at $[x(0), y(0), \theta(0)] =$ [-1m, 0m, 45°] and the obstacle is located at $(x_o, y_o) = (-1\text{m}, 1.3\text{m})$.

The experimental results are shown as Figs. 8 and 9. From Figs. 8b and 9b, we can see that the tracking errors of the proposed adaptive control algorithm are asymptotically convergent regardless of tracking a linear trajectory or a circular trajectory. In the straight line reference trajectory simulated results, even if the robot is affected by wheels' slipping interference and the obstacle, the mobile robot eventually approaches the reference trajectory with asymptotic stability within 3.5 seconds to 0.5% error bound by the proposed unified controller for tracking and obstacle avoidance In the circular reference trajectory simulated results, the mobile robot eventually approaches the reference trajectory with asymptotic stability within 4.2 seconds to 0.5% error bound Meanwhile, Fig. 8a and 9a all reveal that there is no collision between the robot and obstacle. This fact demonstrates the effectiveness of the proposed unified control method

In both simulation and experimental results, the disturbances caused the collision avoidance and wheels' slipping effect indicates a trajectory that is not subject to a nonholonomic mobile robot. The reason is that collision avoidance has a higher priority than trajectory tracking, as collision among robots could lead to system damage, which is more critical than temporary deterioration of tracking performance. Furthermore, the wheels' slipping effect causes the mobile robot to not meet the nonholonomic constraint.

## 6 Conclusions

In this paper, a unified control approach has been proposed to simultaneously solve the tracking and obstacle avoidance of mobile robots with the wheel's unknown slipping at the kinematic level. The robot kinematic model has been derived from the model without slipping. The AUKF is designed to estimate three slipping parameters online in a noisy environment Meanwhile, a novel unified controller is used to handle tracking and obstacle avoidance for mobile robots has been designed by the Lyapunov design technique. We have designed the control law to compensate for unknown wheels' slipping and have proved the stability of the controlled closed-loop robot system from the Lyapunov stability approach with the potential function. Finally, simulation and experimental results have validated that the proposed controller has good tracking and obstacle avoidance control performance and robustness against the unknown wheels' slipping

**Acknowledgments** This work was supported by the National Natural Science Foundation of China (No.U1404614 No.61503202), the Henan Province Education Department Foundation (No. 14B120003, No.17A413002), the Henan Province Scientific and Technological Foundation of China (No. 152102210336)

## References

1. Lee, T.C., Jiang, Z.P.: Uniform asymptotic stability of nonlinear switched systems with an application to mobile robots. IEEE Trans. Autom. Control **53**(5), 1235–1252 (2008)
2. Bazzi, S., Shammas, E., Asmar, D.: A novel method for modeling skidding for systems with nonholon- omic constraints. Nonlinear Dyn. **76**(2), 1517–1528 (2014)
3. Miao, Z., Wang, Y.: Adaptive control for simultaneous stabilization and tracking of unicycle mobile robots. Asian J. Control **18**(3), 1–12 (2016)
4. Cui, M., Liu, W., Liu, H., et al.: Extended state observer-based adaptive sliding mode control of differential-driving mobile robot with uncertainties. Nonlinear Dyn. **83**(1–2), 667–683 (2016)
5. Sun, D., Hu, S., Shao, X., Liu, C.: Global stability of a saturated nonlinear PID controller for robot manipulators. IEEE Trans. Control Syst. Technol. **17**(4), 892–899 (2009)
6. Miao, Z., Wang, Y., Yang, Y.: Robust tracking control of uncertain dynamic nonholonomic systems using recurrent neural networks. Neurocomputing **142**(1), 216–227 (2014)
7. Park, B.S., Yoo, S.J., Park, J.B., Choi, Y.H.: Adaptive neural slipping mode control of nonholonomic wheeled mobile robots with model uncertainty. IEEE Trans. Control Syst. Technol. **17**(1), 207–214 (2009)
8. Miah, M.S., Gueaieb, W.: RFID-based mobile robot trajectory tracking and point stabilization through on-line neighboring optimal control. J. Intell. Robot. Syst. **78**(3–4), 377–399 (2015)
9. Miah, M.S., Gueaieb, W.: Mobile robot trajectory tracking using noisy RSS measurements: An RFID approach. J. Autom. **53**(2), 433–443 (2014)
10. Duguleana, M., Mogan, G.: Neural networks based reinforcement learning for mobile robots obstacle avoidance. Expert Syst. Appl. **62**(11), 104–115 (2016)
11. Yoo, S.J.: Adaptive neural tracking and obstacle avoidance of uncertain mobile robots with unknown skidding and slipping. Informat. Sci. **238**(7), 176–189 (2013)
12. Uchiyama, N., Hashimoto, T., Sano, S., Takagi, S.: Model-reference control approach to obstacle avoidance for a human-operated mobile robot. IEEE Trans. Ind. Electron. **56**(10), 3892–3896 (2009)
13. Ullah, I., Ullah, F., Ullah, Q., Shin, S.: Integrated tracking and accident avoidance system for mobile robots. Int. J Integrated Control Autom. Syst. **11**(6), 1253–1265 (2013)
14. Quoy, M., Moga, S., Gaussier, P.: Dynamical neural networks for planning and low-level robot control. IEEE Trans. Syst., Man, Cybern. A, Syst. Humans **33**(4), 523–532 (2003)
15. Cui, M., Huang, R., Liu, X., et al.: Adaptive tracking control of wheeled Mobile robots with unknown Longitudinal and Lateral slipping parameters. Nonlinear Dyn. **78**(3), 1811–1826 (2014)

16. Wang, Z.P., Ge, S.S., Lee, T.H.: Adaptive neural network control of a wheeled mobile robot violating the pure nonholonomic constraint. In: Proceeding of the IEEE International Conference on Decision and Control, p. 51985203 (2004)
17. Wang, D., Low, C.B.: Modeling and analysis of skidding and slipping in wheeled mobile robots: control design perspective. IEEE Trans. Robot. **24**(3), 676687 (2008)
18. Low, C.B., Wang, D.: GPS-based path following control for a car-like wheeled mobile robot with skidding and slipping. IEEE Trans. Control Syst. Technol. **16**(2), 340–347 (2008)
19. Hoang, N.B., Kang, H.J.: Neural network-based adaptive tracking control of mobile robots in the presence of wheel slip and external disturbance force. Neurocomputing **188**, 12–22 (2016)
20. Stipanović, D.M., Hokayem, P.F., Spong, M.W., Šiljak, D.D.: Cooperative avoidance control for multiagent systems journal of dynamic systems. Measur. Control **129**(5), 699–707 (2007)
21. Dong, W.: Tracking control of multiple-wheeled mobile robots with limited information of a desired trajectory. IEEE Trans Robot. **28**(1), 262–268 (2012)
22. Do, K.D.: Formation tracking control of unicycle-type mobile robots. IEEE Trans. Control Syst. Technol. **16**(3), 527–538 (2008)
23. Yoo, S.J.: Adaptive-observer-based dynamic surface tracking of a class of mobile robots with nonlinear dynamics considering unknown wheel slippage. Nonlinear Dyn. **81**(4), 1611–1622 (2015)
24. Yoo, S.J.: Adaptive tracking and obstacle avoidance for a class mobile robots in the presence of unknown skidding and slipping. IET Control Theory Appl. **5**(14), 1597–1608 (2011)
25. Zhou, B., Han, J., Dai, X.: Backstepping based global exponential stabilization of a tracked mobile robot with slipping perturbation. J. Bionic Eng. **8**(1), 69–76 (2011)
26. Brunke, S., Campbell, M.: Estimation architecture for future autonomous vehicles. In: American Control Conference, IEEE Proceedings of 2002, vol. 2, pp. 1108–1114 (2002)
27. Cui, N.Z., Hong, L., Layne, J.R.: A comparison of nonlinear filtering approaches with an application to ground target tracking. Signal Process. **85**(8), 1469–1492 (2005)
28. Lefebvre, T., Bruyninckx, H., De Schutter, J.: A new method for the nonlinear transformation of means and covariances in filters and estimators. IEEE Trans. Autom. Control **45**(3), 477–482 (2000)
29. Sun, F., Hu, X., Zou, Y., Li, S.: Adaptive unscented Kalman filtering for state of charge estimation of a lithium-ion battery for electric vehicles. J. Energy. **36**(5), 3531–3540 (2011)
30. Song, Q., Han, J.D.: An adaptive UKF algorithm for the state and parameter estimations of a mobile robot. Acta Autom. Sinica. **34**(1), 72–79 (2008)
31. Cui, M., Sun, D., Liu, W., Zhao, M., Liao, X.: Adaptive tracking and obstacle avoidance control for mobile robots with unknown sliding. Int. J. Adv. Robot. Syst. **9**(171), 1–14 (2012)
32. Yang, H., Fan, X., Shi, P., Hua, C.: Nonlinear control for tracking and obstacle avoidance of a wheeled mobile robot with nonholonomic constraint. IEEE Trans. C.ntrol Syst. Technol. **24**(2), 741–746 (2016)
33. Mamadou, M., Cédric, J., Michel, F.: Numerical differentiation with annihilators in noisy environment. Numer. Algorithm. **50**(4), 439–467 (2009)

**Mingyue Cui** received his B.S. degree in automation engineering from Luoyang University of Science and Technology, Luoyang, China, in 1997; the M.S. degree in control theory and control engineering from Lanzhou University of Technology, Lanzhou, China, in 2009; and the Ph.D. degree in control theory and control engineering from Chonqging University, Chongqing, China, in 2012, respectively. He is currently an associate professor of control science and engineering with Nanyang Normal University, Nanyang, China. His current research interests include nonlinear control, and mobile robot control.

**Hongzhao Liu** received the B.S. and M.S. degrees in College of Electric Engineering and Automatic from Henan Polytechnic University, Jiaozuo, China, in 2004 and 2007, respectively, where he is currently pursuing the Ph.D. degree with the College of Automation from Chongqing University. His current research interests include robotics, nonlinear systems and control, and adaptive control.

**Wei Liu** received the B.S. and M.S. degrees from the Department of Automation, Zhengzhou University, Zhengzhou, China, in 2006 and 2009 respectively, and the Ph.D. degree from the Institute of Automation, Chinese Academy of Sciences, Beijing, in 2012. He is currently an Assistant Professor in Nanyang Normal University, Nanyang, China. His research interests include artificial intelligence and pattern recognition.

**Yi Qin** received the B.S. degree in electronics from Information Science and Technology College, Beijing Institute of Technology, Beijing, China, and the M.S. degree in Jinan University, China, in 2004 and 2010, respectively. He is currently a vice Professor in Nanyang Normal University, Nanyang, China. His current research interests include digital image processing and optical information processing.